FEMopt Studios

Acoustic Emission Analysis and Optimization with XCARAT

White Paper, March, 2024

XCARAT

This software includes both a finite element (FE) solver and a structural optimizer for calculation and optimization purposes. It allows for the integration of structural optimization methods, such as shape or topology optimization, into various internal workflows for simulation, pre- and post-processing. For this, standard objective functions such as stiffness, stress or mass can be used and individual solutions can be integrated via the Python interface.

Abstract

Considering acoustic emission when designing a component under dynamic loads can help to reduce development time and improve design effectiveness. This white paper presents how XCARAT can be used to analyze and optimize components in terms of acoustic emission. The methodology implemented for this purpose is described in detail, and the available acoustic structural response for optimization are explained. A simple thin plate structure demonstrates the effectiveness of acoustic analysis and optimization. Thereby, the shape optimization method is used to find optimal bead structures, and the thickness optimization method is used to find suitable distributions of damping material layers. As a result, all the design proposals found show reduced acoustic emission. Whereby, one method of structure optimization is suitable for pushing the excitation frequencies out of a certain range, while the second method reduces the noise by increasing the damping.

Content

Introduction

The acoustic emission (emission of sound) from dynamically excited components, such as gear casings or thin sheet structures of large household appliances is playing an increasing role in their design process. On the one hand, the resulting noise constitutes a crucial selling point, while on the other hand, the propagation of associated acoustic waves (pressure and density fluctuations) can interact with other structures, inducing vibrations in them as well. This often occurs only at specific operating points or within certain frequency ranges. When this knowledge is incorporated into the design process, the methods of structural acoustics (Sinambari, 2017) can be employed to influence the resulting sound development of the components. A highly effective method is structural optimization, through which the geometry or material damping of the component can be optimized to reduce the propagation of structure-borne sound and consequently minimize sound emission.

The software XCARAT (FEMopt Studios GmbH, 2022) can be a valuable tool in such a design process in two ways. Firstly, based on a harmonic analysis (Katznelson, 2012), it can determine the pure sound emission (structure-borne sound) of the component surface (without considering physical effects from near and far fields). This approach allows for the identification of acoustic weak points. Secondly, using the acoustic emission analysis, optimization can be performed by altering the geometry of the component to reduce sound emission in a specified frequency range (shape optimization) or by determining an optimal distribution of a damping material layer on a surface (thickness optimization). Thereby, the method of shape optimization can be used to find optimal shapes of beads.

The focus of this white paper is to demonstrate the functionality of acoustic emission analysis and the effectiveness of acoustic structural optimization using a square perforated plate. The methods of shape optimization and thickness optimization are employed to illustrate their impact on the design process.

Structural Model

Figure 1 shows the geometry and boundary conditions of a thin square plate. The structural model, which is harmonically excited in the frequency range of 50-150 Hz, has dimensions of a x a, with a = 1000.0 mm, and features a circular cutout with a radius of r = 125 mm. Due to discretization, the model consists of 4441 linear shell composite elements. The translational degrees of freedom of all four edges are locked (Navier support). The structural model is continuously excited across the frequency range with a force in z-direction of 0.01 N in the highlighted area of Figure 1. For the optimizations, a linear elastic isotropic material is used for both the thin sheet (with a thickness of 0.5 mm) and the damping material layer (with a thickness of 1.0 mm). The metal plate (layer 1) has an elastic modulus E of 2.0e+5 N/mm², a density ρ of 7.81e-9 t/mm³, and a Poisson's ratio η of 0.3. The damping material layer (layer 2) possesses a damping factor DMPS of 0.2, E of 5.0e+3 N/mm², ρ of 2.45e-9 t/mm³, and η of 0.3.

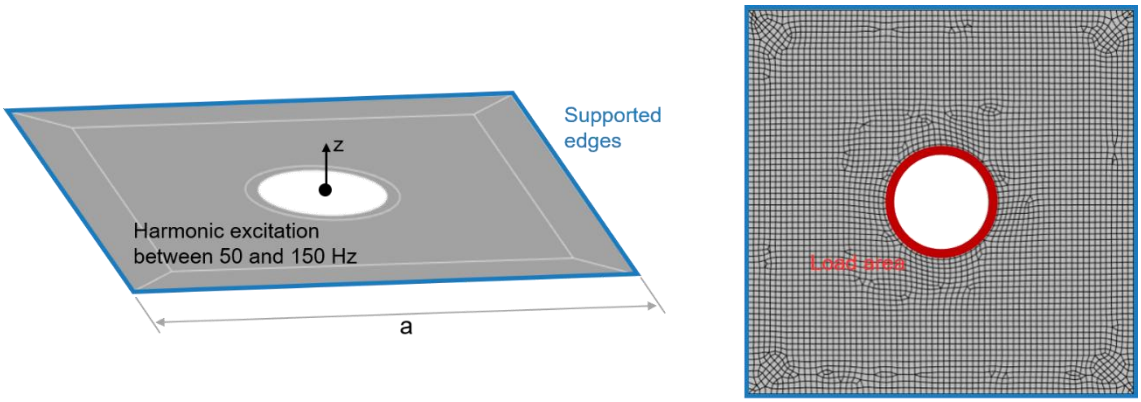

Figure 1: CAE model and FE model square perforated plate

Acoustic Emission Analysis

This analysis facilitates the computation of sound emission from a harmonically oscillating structure based on a preceding frequency response analysis (Chau, 2012). In this way, the response of a structure to a harmonic excitation in the steady state is determined:

$$(-\Omega^2 \boldsymbol{M}(\boldsymbol{s}) + i\Omega \boldsymbol{C}(\boldsymbol{s}) + \boldsymbol{K}(\boldsymbol{s})) \cdot \boldsymbol{u}^+ = \boldsymbol{f}^+, \tag{1}$$

where Ω represents the angular frequency, $\boldsymbol{s}$ the design variable vector, $\boldsymbol{M}$ the mass matrix, $\boldsymbol{C}$ the damping matrix, $\boldsymbol{K}$ the elastic stiffness matrix of the optimization model, $\boldsymbol{u}^+$ the resulting complex displacement vector and $\boldsymbol{f}^+$ the complex vector of the external forces. The outcomes encompass response quantities, typically deformation amplitudes, presented as a curve across the frequencies f_i within the investigated frequency band. The subsequent acoustic emission analysis results in the total sound emission of the structure across the frequency band utilized for the frequency response analysis.

The central parameter for calculating the sound emission is the squared sound particle velocity, v_n^2 [m²/s²]. To achieve this, the normal velocity component v_n [m/s] per FE node of the oscillating surface is calculated based on the displacement amplitude from the harmonic analysis and the angular frequency Ω. Afterwards, these values are then averaged in time and space.

The squared sound particle velocity can be used to calculate the emitted radiated power, ERP [W]. This is a widely accepted criterion for evaluating structure-borne sound:

$$ERP = {}^1\!/_2 \cdot \rho \cdot c \cdot \sigma \cdot A_{total} \cdot v_n^2(f_i), \tag{2}$$

where σ represents the emission rate, ρ denotes the density, and c denotes the sound speed of the fluid (in this case air) and A_{total} the total area of the emitting surface. Due to the use of a constant emission rate $\sigma = 1$, the ERP value constitutes an estimation of the radiated structure-borne sound power. Based on this, the sound power level L_w [dB] can subsequently be determined using a reference power level $p_0 = 10^{-12}$ [W] and the decimal logarithm of the Bel scale:

$$L_w = 10 \cdot \log\left(\frac{ERP}{p_0}\right). \quad (3)$$

Figure 2 illustrates the result of the acoustic emission analysis of the previously described model of the square perforated plate across the frequency range of 50-150 Hz. In this calculation, the sound power level L_w was set as the output parameter. In XCARAT, further acoustic outputs v_n, v_n^2 and ERP are available. The diagram shows that the radiated structure-borne sound power of the whole surface decreases as the frequency increases. Additionally, it shows that five frequencies within the defined frequency band cause the model to vibrate particularly strong.

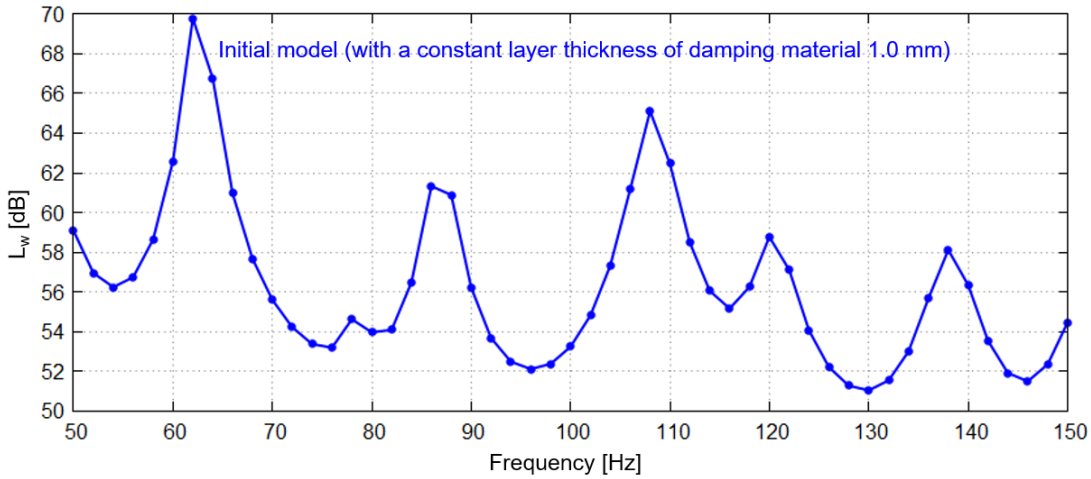

Figure 2: Sound power level of the square perforated plate with the frequency range of 50-150 Hz (average sound power level of 56.33 dB)

Optimization Procedures

An optimization step may be done based on the results of the acoustic emission analysis. This involves performing an acoustic emission analysis for each optimization iteration. Therefore, XCARAT provides an acoustic response function that can be used both as an objective function and as a constraint. For the computation of the acoustic structural response (4), a more general formulation is currently included that requires only the square sound particle velocity. This function consists of two parts: the first part encompasses the logarithmic sum of all emissions within the frequency spectrum, while the second part considers only the maximum value. Both parts, as evident in Equation (4), are multiplied by a weighting factor:

$$f(\boldsymbol{s}) = w_{average} \cdot \sum_i log\left(\breve{v}_n^2(f_i)\right) + w_{peak} \cdot max_i\left(\breve{v}_n^2(f_i)\right). \quad (4)$$

Since a gradient-based optimization algorithm is implemented in XCARAT, the algorithm computes information from iteration to iteration to determine the design update. This information is provided by the calculated sensitivities (gradients), which are determined by discrete sensitivity analysis using the adjoint method for each design variable (Daoud, 2005). Various filtering methods can be used to further smooth the resulting gradient field. Based on the gradients and the status of the defined constraints, a new search direction is determined for all design variables using the Augmented Lagrange Multiplier method.

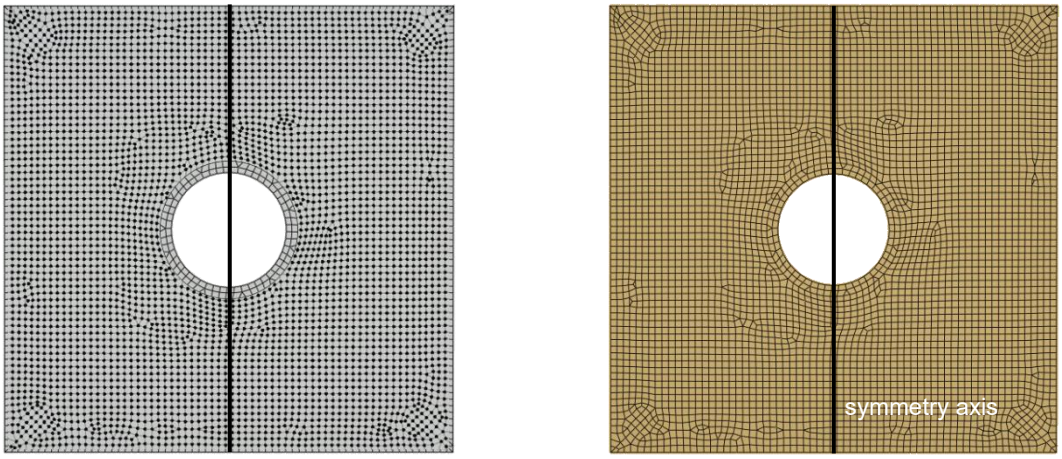

Figure 3: Overview of design variables (nodes) for shape optimization on the left side and design variables (thickness layer 2) for sizing optimization with an initial layer thickness of 1.0 mm on the right side

Shape Optimization

The general goal of this subfield of structural optimization is to find an optimal external shape of a component with respect to the chosen optimization formulation. For this purpose, the defined design variables $\boldsymbol{s}$, which describe the contour of the structure, are varied. The overall topology of the part is maintained, so no holes are created.

Specifically, in XCARAT, a finite element (FE) mesh-based approach is implemented, where each surface node of a pre-defined node set corresponds to a design variable (parameter-free shape optimization) (Firl, 2010). This type of shape optimization requires the use of mesh regularization techniques that can affect the quality of the FE mesh both in the plane and orthogonal to the surface (Firl, et al., 2013). Consequently, the FE results are not falsified, and the FE mesh remains intact. In XCARAT, the orthogonal displacement of nodes is controlled by filtering the respective gradients, and the tangential displacement is managed through the implemented Minimal Surface Regularization method.

Regarding the optimization model in Figure 1, all the nodes marked on the perforated plate in Figure 3 (exclude the supported edges and the loading area) can be modified by the algorithm according to the defined optimization problem to minimize the response function $f(\boldsymbol{s})$, so that the separate design variables s_i do not violate the variable bound $-20.0\,mm \leq s_i \leq 20.0\,mm$.

Thickness Optimization

This type of optimization is part of parameter optimization, where only the thickness of a component or layer is varied. This approach allows for the discovery of optimal thickness distributions for thin sheet structures or beams with respect to applied loads.

Within the context of acoustic optimization, for example, the thickness of a damping material layer can be optimized. This use case is also applied to the perforated plate model. For this purpose, a proven modeling method, which has already been described in the Model section, is utilized. This allows for a simple layered structure of the model, where the first layer represents the thin metal sheet, and the second layer represents the damping material.

For the optimization of the right model in Figure 3, the goal is to minimize $f(\boldsymbol{s})$ while maintaining the initial mass (equally mass constraint). Thereby, the design variables may assume values between $0.1\,mm \leq s_i \leq 2.0\,mm$.

Optimization Results

The optimization tasks defined in the Shape Optimization and Thickness Optimization sections were performed with the acoustic structural response (4), specifically using only the first part of the equation ($w_{average} = 1$ and $w_{peak} = 0$). The gradients generated at each optimization step were smoothed using the default setting of the linear filter (for this case a filter radius of 44.2 mm). Additionally, a symmetry boundary condition with respect to the axis indicated in Figures 3 was active.

After 125 iterations, the algorithm has reached a local minimum for shape optimization. As shown in Figure 4, the axisymmetric bead structure converges toward the variable bounds $-20.0\,mm \leq s_i \leq 20.0\,mm$.

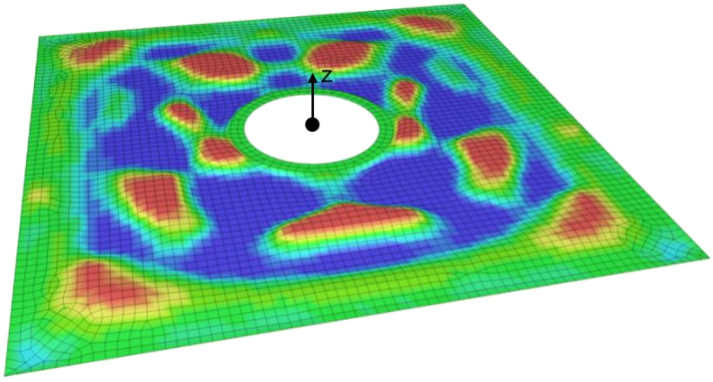

Figure 4: Resulting bead structure of the shape optimization after 125 iterations
(Legend z direction: -20.0 mm | 0 mm | 20.0 mm)

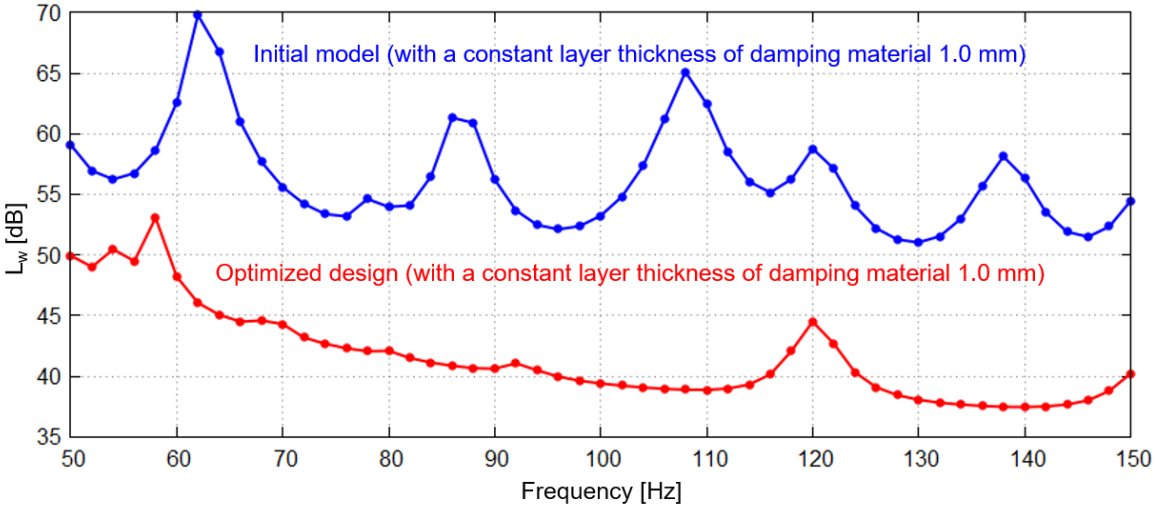

Figure 5: Resulting sound power level of the bead structure having average sound power level of 41.58 dB

Figure 5 illustrates the impact of the optimal solution on structure-borne sound radiation. Compared to the initial curve, the level of structure-borne sound radiation is lower overall, and there are only two smaller peaks in the considered frequency range.

In terms of the average sound power level of 41.58 dB, this represents an improvement of 26.2 %. Furthermore, it is observed that the bead structure introduces significantly more stiffness into the model. As a result, the frequencies that particularly strongly excite the system are shifted out of the range of 50-150 Hz.

In the thickness optimization, the algorithm converged after 150 iterations. Figure 6 displays a distribution of the damping material layer, occupying a maximum allowable 50% of the design space, as shown.

As evident from Figure 7, the solution obtained results in a significantly higher damping in the system. Consequently, the average sound power level is reduced by 11.0 % to 50.20 dB. The optimal distribution of the damping material layer not only reduces the maximum peaks of structure-borne sound radiation but also shifts regions of maximum excitation to other frequency ranges. This is attributed to the localized distribution of the material layer and the associated alteration of stiffness in the system.

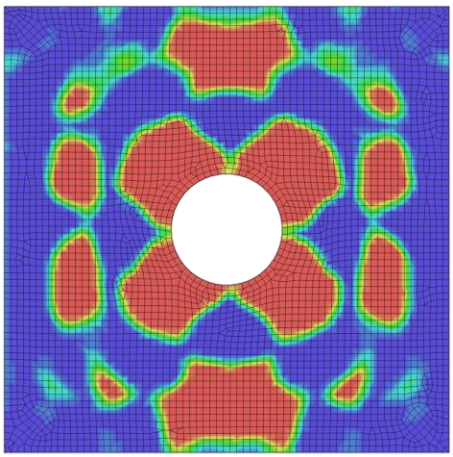

Figure 6: Resulting layer distribution of the thickness optimization after 150 iterations (Legend thickness: 0.1 mm | 1.0 mm | 2.0 mm)

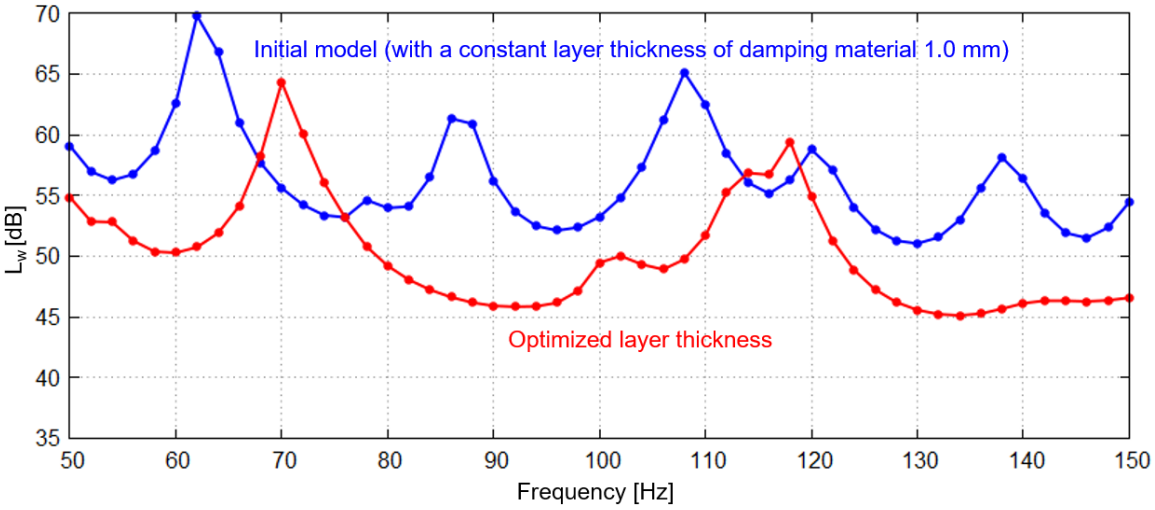

Figure 7: Resulting sound power level of the square perforated plate with the optimized thickness distribution having average sound power level of 50.20 dB

Conclusion

The presented methodology and the results of the optimizations illustrate how this approach can make the design process of dynamically excited components more effective in terms of reducing structure-borne sound. Additionally, noise-generating components of an assembly can be identified and revised promptly using this method.

In general, two points can be emphasized. Firstly, beading the component surface leads to stiffening, which shifts frequencies out of a certain range. Conversely, the addition of an extra material layer to the component introduces more damping and stiffness into the system, thereby reducing acoustic emission. Secondly, the optimizations have shown that they lead to acoustically meaningful solutions capable of reducing the originally induced structure-borne sound.

References

Chau, P. C., 2012. *Process Control.* s.l.:Cambridge University Press.

Daoud, F., 2005. *Formoptimierung von Freiformschalen Mathematische Algorithmen und Filtertechniken.* s.l.:s.n.

DIN EN 61672-1:2014-07, 2013. *Elektroakustik – Schallpegelmesser – Teil 1: Anforderungen (IEC 61672-1:2013); Deutsche Fassung EN 61672-1:2013,* s.l.: Beuth Verlag GmbH.

FEMopt Studios GmbH, 2022. *Product side of FEMopt homepage.* [Online] Available at: https://femopt.de/en/product/ [Accessed Januar 2024].

Firl, M., 2010. *Optimal shape design of shell structures.* s.l.:s.n.

Firl, M., Wüchner , R. & Bletzinger, K.-U., 2013. Regularization of shape optimization problems using FE-based parametrization. *Structural and Multidisciplinary Optimization,* Issue 47, p. 507–521.

Katznelson, Y., 2012. *An introduction to harmonic analysis.* 3 ed. s.l.:Cambridge University Press .

Sinambari, G. R., 2017. *Konstruktionsakustik - Primäre und sekundäre Lärmminderung.* 1 ed. s.l.:Springer Vieweg Wiesbaden.